

ADHint: Adaptive Hints with Difficulty Priors for Reinforcement Learning

Feng Zhang^{1,2*}, Zezhong Tan^{1,3*}, Xinhong Ma¹, Ziqiang Dong^{1**}, Xi Leng^{1,4},
Jianfei Zhao^{2,5}, Xin Sun², and Yang Yang¹

¹ Alibaba Group ² Beijing Institute of Technology ³ Peking University
⁴ The Chinese University of Hong Kong, Shenzhen ⁵ Zhongguancun Academy
{xinhong.mxh, ziqiang.dzq, chris.yang}@alibaba-inc.com
{bit_zhangfeng, zhaingan, sunxin}@bit.edu.cn
tzz@stu.pku.edu.cn, 221019056@link.cuhk.edu.cn

Abstract. To address the limited capability expansion and low sample efficiency of Reinforcement Learning (RL), recent methods have integrated “hints” into post-training, which are prefix segments of complete reasoning trajectories, aiming for powerful knowledge expansion and reasoning generalization. However, existing hint-based RL methods often neglect the role of difficulty in the hint-ratio schedule and relative-advantage estimation, resulting in unstable learning and excessive imitation of off-policy hints. To address this, we propose ADHint, which explicitly integrates difficulty into both processes to achieve a better trade-off between exploration and imitation. Specifically, we propose **Adaptive Hint with Sample Difficulty Prior**, which evaluates the difficulty of each sample under the current policy to schedule an appropriate hint ratio for rollout generation. Furthermore, we introduce **Consistency-based Gradient Modulation** alongside **Selective Masking for Hint Preservation**, which jointly modulate token-level gradients within hints to prevent biased and destructive updates. Additionally, we propose **Advantage Estimation with Rollout Difficulty Posterior**, which leverages the relative difficulty of rollouts with and without hints to compute their respective advantages, yielding more balanced updates. Extensive experiments across diverse modalities, model scales, model families, and domains demonstrate that ADHint achieves superior reasoning capabilities and out-of-distribution generalization. Code and datasets will be made publicly available upon paper acceptance.

Keywords: Adaptive Hints · Reinforcement Learning · Difficulty Priors

1 Introduction

Recent advancements in Large Language Models (LLMs) [19, 47, 48, 53] and Multimodal Large Language Models (MLLMs) [1, 13, 26, 39] highlight the potential

* Equal contribution.

** Corresponding author.

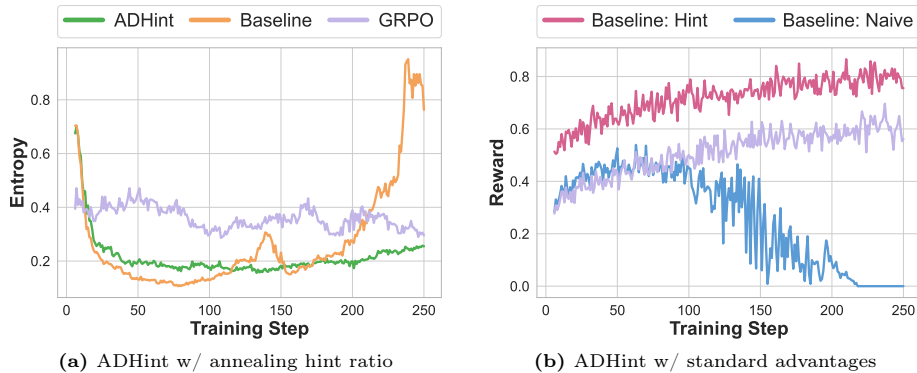


Fig. 1: Baseline behavior with existing hint-based designs. “ADHint w/ annealing hint ratio” replaces our sample difficulty prior-based hint-ratio schedule (AH-SDP) with a commonly used time-varying schedule. “ADHint w/ standard advantages” replaces our rollout difficulty posterior-based advantage estimation (AE-RDP) with the standard estimation that pools hint-rollouts and naive-rollouts into a single GRPO group. In each subfigure, the *Baseline* curve matches the variant in the title, and “Baseline: Hint/Naive” reports statistics from hint- or naive-rollouts only.

to enhance reasoning capabilities by large-scale Reinforcement Learning with Verifiable Rewards (RLVR) [8, 33, 50], such as Proximal Policy Optimization (PPO) [32] and Group Relative Policy Optimization (GRPO) [8, 33]. However, current on-policy RLVR faces two major challenges: (1) *Limited capability expansion*: RLVR is inherently bounded by the base model. It primarily amplifies existing behaviors and refines known reasoning chains, rather than instilling genuinely novel reasoning abilities beyond its initial capability boundaries [5, 19]. (2) *Low sample efficiency*: The learning process is bottlenecked by the current policy’s performance, yielding critically sparse reward signals that render hard samples difficult to exploit [42, 43].

To mitigate these limitations, recent methods [12, 22] introduce *hints*, defined as prefix segments of complete reasoning trajectories, which guide the policy to explore the continuation, thereby acquiring novel capabilities and solving challenging problems. Specifically, these methods assign fixed [54] or time-varying [14, 22] hint ratios to all samples (or only to the hardest samples [12, 25]), and then utilize *hint-rollouts* derived from hint-guided reasoning together with *naive-rollouts* generated without hints for group relative advantage estimation [14, 54].

Despite their empirical successes, existing hint-based RL methods are sensitive to sample-difficulty in the hint-ratio schedule and rollout-difficulty in the relative-advantage estimation. Specifically, most previous methods apply a uniform hint ratio to both easy and hard samples for model reasoning, and then generate hint-rollouts with various difficulties. Policy learning from such heterogeneous rollouts could introduce high-variance model optimization, and thus undermine training stability [3, 17, 29]. As shown in Figure 1a, the model with annealing hint ratio (denoted as Baseline) suffers from training collapse since its entropy rises sharply at the end of training, indicating insufficient absorption of external knowledge and a drift in the model’s own policy. In contrast, when

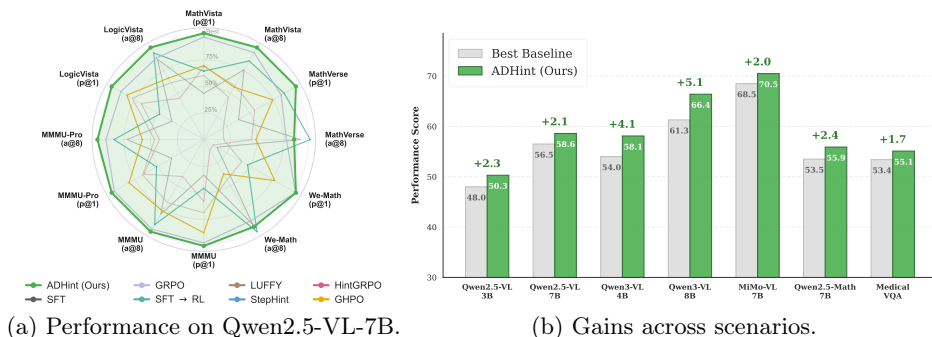


Fig. 2: Performance Comparison and Generalization. (a) Radar chart on Qwen2.5-VL-7B-Instruct. Each axis represents a dataset-metric pair ($p@1$: $pass@1$, $a@8$: $avg@8$), where ADHint consistently achieves the best or highly competitive performance. (b) Absolute gains over the best baselines. ADHint demonstrates robust improvements across diverse modalities, model scales, model families, and domains.

incorporating the hint-ratio schedule with sample-difficulty (our method, discussed later), the entropy converges stably, ensuring that the model internalizes robust reasoning abilities rather than superficial patterns within off-policy hints.

As for relative-advantage estimation, most existing approaches pool hint-rollouts and naive-rollouts into a single group so that the relative-advantage is dominated by hint-rollouts, with the model learning to directly imitate the off-policy hint distribution rather than exploring with its own policy under hint guidance. Specifically, externally guided hint-rollouts are typically simpler than naive-rollouts, leading to more trajectories with positive advantages that dominate the update signal and bias the policy toward fitting the off-policy distribution. Additionally, hints from external reasoning models are usually much longer than the policy’s own outputs, further exacerbating this imbalance. As shown in Figure 1b, the average reward of hint-rollouts increases steadily, whereas that of naive-rollouts collapses, causing the model (denoted as Baseline) to eventually lose the ability to perform inference without hints.

To address these issues, we propose **ADHint** (**AD**aptive **H**ints with **D**ifficulty **P**riors for Reinforcement Learning), which incorporates difficulty into both the hint-ratio schedule and the relative-advantage estimation to achieve a principled trade-off between exploration and imitation. For the hint-ratio schedule, we propose **Adaptive Hint with Sample Difficulty Prior** (AH-SDP), which adaptively determines the hint ratio for each sample based on a difficulty prior estimated from the average reward of its naive-rollouts, maintaining the resulting hint-rollouts within a moderate difficulty range to provide stable update signals. Furthermore, to prevent drastic shifts toward the off-policy distribution that trigger entropy collapse, we propose **Consistency-based Gradient Modulation** (CGM), which downweights the gradients of hint tokens whose entropy deviates significantly from that of the policy-generated continuation. We also introduce **Selective Masking for Hint Preservation** (Selective Masking), which discards erroneous update signals from hint-rollouts with negative advantages. For the relative-advantage estimation, we propose **Advantage Estimation with**

Rollout Difficulty Posterior (AE-RDP), which constructs the rollout difficulty posterior from the average rewards of both naive-rollouts and hint-rollouts, and uses it to estimate advantages. Positive naive-rollouts with greater difficulty receive larger advantages, as they provide valuable learning signals better aligned with the current policy, whereas negative hint-rollouts with lower difficulty are penalized more heavily.

We conduct extensive experiments across multiple modalities, model scales, model families, domains, and tasks. As shown in Figure 2, ADHint consistently yields substantial gains, demonstrating synergistic improvements in both reasoning ability and out-of-distribution generalization. Our main contributions are summarized as follows:

- We reveal that difficulty is a crucial signal for both the hint-ratio schedule and relative-advantage estimation, and that neglecting it results in unstable learning and overfitting to the off-policy distribution.
- We propose ADHint, which explicitly exploits sample difficulty priors and rollout difficulty posteriors for the hint-ratio schedule and relative-advantage estimation, leading to a better balance between exploration and imitation.
- Extensive experiments across diverse settings consistently demonstrate ADHint’s superiority, delivering robust and significant performance gains across comprehensive multi-domain benchmarks.

2 Related Work

2.1 Multimodal Reinforcement Learning

GRPO [8, 33] removes the critic network from PPO [32] and estimates advantages via intra-group sampling, serving as a cornerstone for recent reasoning models [35–37, 40, 47, 49, 53]. In parallel, the multimodal community has explored various strategies to enhance MLLM reasoning, including refining reasoning styles [34, 38, 59], improving rollout procedures for training robustness [23, 41], redesigning reward functions [24, 26], and augmenting training data [18, 21]. Despite these advances, RL algorithms mainly unlock the latent potential of pre-trained models and often fail to expand their fundamental capability boundary.

2.2 Reinforcement Learning with Off-policy Hints

Recent works incorporate off-policy hints into RL-based post-training by providing partial solution prefixes from off-policy data to guide the model’s reasoning while preserving on-policy exploration. UFT [22] and Prefix-RFT [14] employ temporally annealed hint ratios, whereas StepHint [54] mixes hint-rollouts at multiple hint ratios with naive-rollouts and ground-truth trajectories within a single group. SEELE [20] introduces learnable parameters to predict instance-specific hint ratios in a multi-round training scheme. Other methods reserve hints exclusively for the most challenging samples and determine the hint ratio via uniform sampling [4], binary search [57], or progressive search [12, 25]. In this

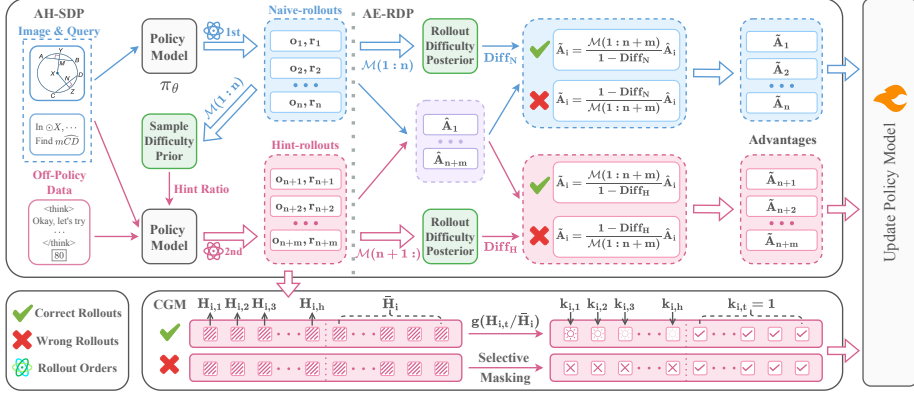


Fig. 3: An overview of ADHint. For each sample, ADHint successively infers twice to obtain naive-rollsouts and hint-rollsouts, where the hint ratio of the latter is scheduled based on the difficulty evaluated from the former. It then leverages the relative difficulty of naive-rollsouts and hint-rollsouts to estimate their respective advantages, and modulates the gradient of each hint token based on the consistency of entropy.

work, we propose ADHint, which explicitly incorporates difficulty into both the hint-ratio schedule and the relative-advantage estimation to address the unstable learning and excessive imitation observed in existing hint-based methods. More detailed discussions are provided in Appendix C.

3 Preliminary

3.1 Group Relative Policy Optimization

For each query q in the question set Q , GRPO samples a group of rollouts $\{o_1, \dots, o_G\}$ from the old policy model $\pi_{\theta_{\text{old}}}$, and computes their respective rewards $\{r_1, \dots, r_G\}$. The current policy model π_θ is optimized by maximizing the following objective:

$$\mathcal{J}_{\text{GRPO}}(\pi_\theta) = \mathbb{E}_{q \sim Q, \{o_i\}_{i=1}^G \sim \pi_{\theta_{\text{old}}}(\cdot|q)} \frac{1}{G} \sum_{i=1}^G \frac{1}{|o_i|} \sum_{t=1}^{|o_i|} \left\{ \frac{\pi_\theta(o_{i,t}|q, o_{i,<t})}{\pi_{\theta_{\text{old}}}(o_{i,t}|q, o_{i,<t})} \hat{A}_i - \beta D_{\text{KL}}(\pi_\theta \| \pi_{\text{ref}}) \right\}$$

where the standard *min* and *clip* operations for avoiding extreme gradients are omitted for clarity, and $D_{\text{KL}}(\pi_\theta \| \pi_{\text{ref}})$ is a KL constraint term. \hat{A}_i is the relative advantage, calculated by normalizing the reward within the group:

$$\hat{A}_i = \frac{r_i - \text{mean}(\{r_1, \dots, r_G\})}{\text{std}(\{r_1, \dots, r_G\})}.$$

The gradient for a given q and o_i is calculated as:

$$\nabla_\theta \mathcal{J}_{\text{GRPO}}^*(\pi_\theta) \Big|_{q, o_i} = \frac{1}{G \cdot |o_i|} \sum_{t=1}^{|o_i|} \frac{\pi_\theta(o_{i,t}|q, o_{i,<t})}{\pi_{\theta_{\text{old}}}(o_{i,t}|q, o_{i,<t})} \cdot \hat{A}_i \cdot \nabla_\theta \log(\pi_\theta(o_{i,t}|q, o_{i,<t})).$$

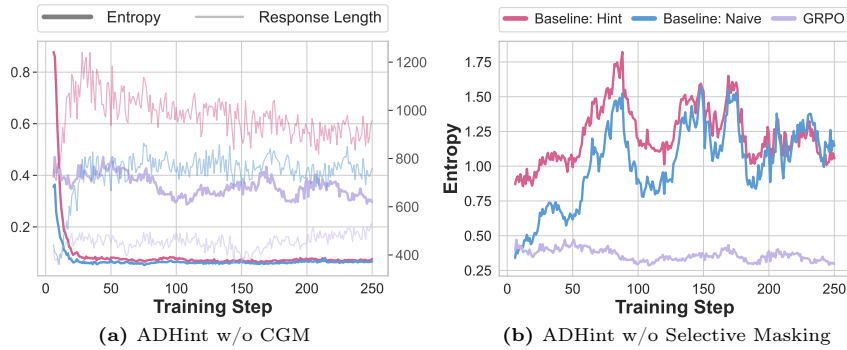


Fig. 4: Baseline behavior after removing CGM or Selective Masking. The left subfigure shows the baseline’s entropy (left axis) and response length (right axis). The right subfigure compares the entropy of the baseline and GRPO, where “Baseline: Hint/Naive” is computed on hint- or naive-rollouts only.

3.2 Hint-based On-Policy Learning

Recent works use the initial part of off-policy reasoning trajectories from a teacher model as *hints* to guide rollouts. Given a query q , a hint ratio w specifies the prefix length h copied from the off-policy trajectory. Conditioned on q , the policy model π_θ then produces two types of rollouts:

- **Naive-rollouts:** Generate n rollouts $\{o_1, \dots, o_n\}$ without guidance, each sampled as $o_i \sim \pi_\theta(\cdot | q)$.
- **Hint-rollouts:** Generate m rollouts $\{o_{n+1}, \dots, o_{n+m}\}$ with hint guidance, each formed as $o_i = [o_{i,<h}; o_{i,>h}]$, where $o_{i,<h}$ is the hint prefix of length h and $o_{i,>h}$ is the continuation sampled as $o_{i,>h} \sim \pi_\theta(\cdot | q, o_{i,<h})$.

In standard practice, the $n+m$ rollouts are pooled into a single group to compute relative advantages. Notably, since hint tokens ($t \leq h$) are not generated by the policy model, following prior work [46], we set $\pi_{\theta_{\text{id}}}(o_{i,t} | q, o_{i,<t}) = 1$ for all hint tokens in hint-rollouts.

4 Method

4.1 Overview

As shown in Figure 3, ADHint comprises four crucial modules: (1) **Adaptive Hint with Sample Difficulty Prior (AH-SDP)**, where the policy model successively performs two inferences to obtain naive-rollouts and hint-rollouts, and accordingly schedules the hint ratio for the latter based on the sample difficulty prior evaluated from the former; (2) **Advantage Estimation with Rollout Difficulty Posterior (AE-RDP)**, which uses the rollout difficulty posterior to estimate relative advantages for naive-rollouts and hint-rollouts, covering both correct and wrong outcomes; (3) **Consistency-based Gradient Modulation (CGM)**, where the gradient of each hint token is modulated according to the consistency of its entropy distribution with that of the continuation; and (4)

Selective Masking for Hint Preservation (Selective Masking), which masks the update signals of hint tokens in hint-rollouts that remain incorrect even with guidance. Additionally, Algorithm 1 summarizes the overall procedure.

4.2 Adaptive Hint with Sample Difficulty Prior

Assigning the same hint ratio to every sample in the current update batch [14, 22, 54] introduces a mismatch in the difficulty of hint-rollouts across samples, yielding unstable training signals and reducing learning efficiency. As shown in Figure 1a, while the entropy drops rapidly in the early stage, it rises sharply in the later phase as the hint ratio becomes low. These observations suggest that the model tends to memorize superficial hint patterns rather than internalize the underlying knowledge.

Unlike existing methods, we use the difficulty prior evaluated from each sample’s naive-rollouts to schedule the hint ratio, thereby keeping hint-rollouts within a moderate-difficulty regime (Figure 5a) and providing low-variance update signals at every step. For each query q , we define the difficulty score of naive-rollouts as

$$\text{Diff}_N = 1 - \mathcal{M}(1 : n) = 1 - \text{mean}(r_1, \dots, r_n). \quad (1)$$

We then compute the hint ratio w using a linear function:

$$w = f(\text{Diff}_N) = (w_{\max} - w_{\min}) \cdot \text{Diff}_N + w_{\min} + \sigma. \quad (2)$$

where w_{\max} and w_{\min} denote the maximum and minimum ratios, and $\sigma \sim \mathcal{U}(-R, R)$ is uniformly distributed noise. We fix $w_{\min} = 0$ since easy questions require no hints, thus eliminating it as a hyperparameter.

Finally, the adaptively computed ratio w determines the hint length h , which we then use to generate m hint-rollouts $\{o_{n+1}, \dots, o_{n+m}\}$.

Consistency-based Gradient Modulation. Since off-policy hints can differ substantially from the on-policy model in language style, knowledge structure, and response length, indiscriminately learning from hints risks overfitting to off-policy patterns. As shown in Figure 4a, the entropies of both naive-rollouts and hint-rollouts collapse sharply, and the response length of naive-rollouts quickly approaches that of hint-rollouts, indicating a policy shift toward the off-policy hints. We mitigate this by measuring the consistency between each hint token and the generated continuation that represents the model’s intrinsic distribution, and using this consistency to modulate the gradients of the hint tokens, thereby avoiding destructive distribution shifts in the policy model.

Specifically, for each hint token in a hint-rollout o_i , we define the token-level entropy as

$$H_{i,t} = \mathcal{H}(\pi_\theta(o_{i,t} \mid q, o_{i,<t})), \quad (3)$$

and the average entropy of the policy-generated continuation as

$$\bar{H}_i = \frac{1}{|o_{i,>h}|} \sum_{t=h+1}^{|o_i|} \mathcal{H}(\pi_\theta(o_{i,t} \mid q, o_{i,<t})). \quad (4)$$

We then scale the gradient of each token by

$$k_{i,t} = g(H_{i,t}/\bar{H}_i) \text{ if } 1 \leq t \leq h, \text{ and } 1 \text{ otherwise.}$$

where $g(x; \alpha)$ is a symmetric cosine-based schedule centered at $g(1) = 1$, with a ramp-up on $[\alpha, 1]$ and a ramp-down on $[1, 1/\alpha]$ for $0 < \alpha \leq 1$:

$$g(x; \alpha) = \begin{cases} \sin\left(\frac{\pi}{2} \cdot \frac{x-\alpha}{1-\alpha}\right), & \alpha \leq x \leq 1, \\ \cos\left(\frac{\pi}{2} \cdot \frac{x-1}{1/\alpha-1}\right), & 1 < x \leq 1/\alpha, \\ 0, & \text{otherwise.} \end{cases}$$

Selective Masking for Hint Preservation. Since the adaptively controlled hint-rollouts remain in a moderate-difficulty regime, some trajectories can yield negative advantages. Applying such negative updates to the hint prefix $o_{i,\leq h}$ is counterproductive because this prefix is assumed to be correct. Penalizing it introduces conflicting gradients and destabilizes learning, often triggering an entropy spike as the model’s predictive distribution becomes overly uncertain (Figure 4b). Thus, we selectively mask the gradients of hint tokens in this case:

$$k_{i,t} = \begin{cases} 0, & 1 \leq t \leq h \text{ and } \hat{A}_i \leq 0, \\ g(H_{i,t}/\bar{H}_i), & 1 \leq t \leq h \text{ and } \hat{A}_i > 0, \\ 1, & t > h. \end{cases} \quad (5)$$

To unify the notation, we fix $k_{i,t} = 1$ for naive-rollouts.

4.3 Advantage Estimation with Rollout Difficulty Posterior

When hint-rollouts and naive-rollouts are pooled into a single group to estimate relative advantages [14, 54], the update is often biased toward hint-rollouts, since they typically contain more positive trajectories and longer responses. As shown in Figure 1b, the average reward of hint-rollouts keeps increasing while the reward of naive-rollouts collapses, indicating overfitting to the hint distribution. In this case, the policy improves “text-completion” behavior but sacrifices genuine reasoning ability.

To address this issue, we introduce the rollout difficulty posterior for advantage estimation, which characterizes the relative difficulty between naive-rollouts and hint-rollouts after both rollouts are completed. Our design follows two intuitions. Since naive-rollouts are typically harder and fully generated by the current policy, their positive trajectories provide more informative signals for policy updates. In contrast, hint-rollouts are relatively easier and thus warrant stronger penalties when incorrect.

Specifically, for each query q , we define the difficulty score of naive-rollouts in Eq. 1, and similarly define the difficulty score of hint-rollouts as

$$\text{Diff}_H = 1 - \mathcal{M}(n+1 :) = 1 - \text{mean}(r_{n+1}, \dots, r_{n+m}). \quad (6)$$

Then the difficulty score of rollout o_i is denoted as

$$\text{Diff}_i = \text{Diff}_N \text{ if } 1 \leq i \leq n, \text{ and } \text{Diff}_H \text{ if } n + 1 \leq i \leq n + m.$$

Let \hat{A}_i denote the relative advantage of rollout o_i , estimated by pooling all $n + m$ trajectories. We define a sign indicator $s_i = \text{sgn}(\hat{A}_i)$, where $s_i = -1$ when $\hat{A}_i \leq 0$. Finally, the relative advantages in ADHint are estimated as

$$\tilde{A}_i = \left(\frac{\mathcal{M}(1 : n + m)}{1 - \text{Diff}_i} \right)^{s_i} \hat{A}_i. \quad (7)$$

4.4 Overall Gradient Computation

Building on the above mechanisms, we compute the gradient for a given query q and rollout o_i as:

$$\nabla_{\theta} \mathcal{J}_{\text{ADHint}}^*(\pi_{\theta}) \Big|_{q, o_i} = \frac{1}{G \cdot |o_i|} \sum_{t=1}^{|o_i|} k_{i,t} \cdot \frac{\pi_{\theta}(o_{i,t}|q, o_{i,<t})}{\pi_{\theta_{\text{id}}}(o_{i,t}|q, o_{i,<t})} \cdot \tilde{A}_i \cdot \nabla_{\theta} \log(\pi_{\theta}(o_{i,t}|q, o_{i,<t})). \quad (8)$$

Notably, to avoid inaccurate difficulty prior evaluations caused by formatting errors, we warm up the policy model with GRPO for the first five steps to ensure the model follows the required response format (Figure 5f).

5 Experiments

5.1 Settings

We conduct experiments across multiple modalities, model scales, model families, and domains to validate ADHint’s effectiveness. For common MLLM reasoning tasks (e.g., math and chart reasoning), we evaluate ADHint on Qwen2.5-VL-7B-Instruct [2], Qwen3-VL-8B-Instruct [1], Qwen2.5-VL-3B-Instruct, Qwen3-VL-4B-Instruct, and MiMo-VL-7B-SFT-2508 [45]. We additionally evaluate ADHint on Medical VQA to assess cross-domain generalization, using the Qwen2.5-VL-7B-Instruct backbone. For LLM math reasoning, we use Qwen2.5-Math-7B [48], following the data and experimental settings of GHPO [25].

Training data. For MLLMs, we construct our training data from the ViRL39K dataset [38], which spans multiple domains, including STEM, chart reasoning, document reasoning, and spatial reasoning. We use Qwen3-VL-30B-A3B-Thinking and Qwen3-VL-235B-A22B-Thinking to sample hints, and remove examples that are considered excessively simple for Qwen2.5-VL-7B-Instruct, resulting in a final set of 17K training queries, termed ViRL-Hint17k. For Medical VQA, we use a 15K subset of the PMC-VQA training set [56]. For LLMs, we use NuminaMath-S, a mixture of MATH [10] and NuminaMath-1.5 [11] curated by GHPO. More details are provided in Appendix D.1.

Benchmarks. For MLLMs, we use benchmarks spanning diverse domains, including MathVista [27], MathVerse [55], and We-Math [31] for math reasoning; MMMU [51] and MMMU-Pro [52] for multi-discipline reasoning; and LogicVista [44] for logical reasoning. For Medical VQA, we use the PMC-VQA test set (PMC-Test) [56]. For LLMs, we evaluate on math reasoning benchmarks, including AIME [30], AMC [16], Minerva [15], OlympiadBench [9], and MATH500 [10]. More details are provided in Appendix D.2.

Evaluation Metrics. For MLLMs, we report *pass@1* and *avg@8* for each benchmark [38,41]. *Pass@1* measures the accuracy of a single rollout per sample under greedy decoding, reflecting the model’s out-of-distribution reasoning generalization. *Avg@8* computes the average accuracy over eight rollouts per sample at temperature 1.0, reflecting the model’s robustness and mastery of the underlying knowledge. For Medical VQA, we report *pass@1* [60]. For LLMs, we report either *pass@1* or *avg@32* depending on the benchmark to mitigate potential variance introduced by the small sizes of some datasets [25].

Implementation Details. For MLLMs, we train for 250 steps (about 2 epochs) with a learning rate of 1×10^{-6} . We set the rollout batch size to 128 and the maximum generation length to 8K. For LLMs, we train for 5 epochs with an initial learning rate of 1×10^{-6} , decayed to zero using a cosine schedule with a warm-up phase covering 10% of the total global steps. We set the maximum generation length to 2K. We set w_{\max} to 0.2 for MLLMs and 0.4 for LLMs, and use $\alpha = 0.5$ as the CGM threshold for both. All training is performed on 4 nodes, each equipped with 8 H100 GPUs. Further details are provided in Appendix D.3.

Baselines. We compare ADHint with several baselines: (1) **GRPO**; (2) **SFT**, trained for two epochs on the full training set; (3) **SFT** \rightarrow **RL**, which applies two epochs of SFT followed by GRPO; (4) **LUFFY** [46], which performs on-policy and off-policy updates jointly at each step; (5) **StepHint** [54], which mixes hint-rollouts with multiple hint ratios, naive-rollouts, and ground-truth trajectories into a group for update; (6) **HintGRPO** [12], which progressively increases the hint ratio for the hardest samples to obtain positive trajectories; and (7) **GHPO** [25], which treats hints as part of the query and uses multiple hint ratios for the hardest samples. We note that several baselines crash during training, and for these methods, we report results from the last checkpoint available before the crash. More detailed information about the baselines and their reimplementations is provided in Appendix D.4 and Appendix D.5, respectively.

5.2 Main Results

SOTA performance with MLLMs. As detailed in Tables 1, 4, and 5, ADHint achieves consistent gains across multiple backbones, validating its robust generalization regarding model capabilities, scales, and families. For Qwen2.5-VL models, ADHint consistently outperforms GRPO, yielding overall *pass@1/avg@8* improvements of 2.1%/2.0% at the 7B scale and 2.3%/2.1% at 3B. Against recent

Table 1: Comparative performance on Qwen2.5-VL models. For each benchmark, we report *pass@1* (the first value) and *avg@8* (the second value). The upper block uses Qwen2.5-VL-3B as the base MLLM, while the lower block uses Qwen2.5-VL-7B. The best and runner-up results are highlighted in **bold** and underlined, respectively.

Method	Math Reasoning			Multi-Discipline		Logical	Avg.
	MathVista	MathVerse	We-Math	MMMU	MMMU-Pro	LogicVista	
<i>Base MLLM: Qwen2.5-VL-3B</i>							
SFT	51.9/61.3	31.2/ 54.2	32.5/58.5	28.6/46.3	17.1/29.4	18.1/37.8	29.9/47.9
SFT → RL	53.6/ <u>63.3</u>	37.4/ <u>54.1</u>	38.3/ 60.6	30.6/47.7	18.7/ <u>30.9</u>	18.1/ <u>39.9</u>	32.9/ <u>49.4</u>
GRPO [33]	<u>63.9</u> /63.1	<u>43.1</u> /45.0	<u>59.0</u> /59.0	<u>47.5</u> / <u>49.1</u>	<u>30.7</u> /30.1	43.8 /38.9	<u>48.0</u> /47.5
LUFFY [46]	41.2/45.6	31.7/35.0	42.3/46.1	34.3/44.6	20.3/23.1	35.4/38.3	34.2/38.8
StepHint [54]	34.9/44.6	28.7/32.5	32.0/40.2	18.3/35.7	19.8/26.0	12.5/27.8	24.4/34.5
HintGRPO [12]	56.7/52.5	37.4/39.7	42.0/40.5	44.4/43.0	27.5/25.1	35.7/33.7	40.6/39.1
GHPO [25]	57.3/55.2	35.6/35.4	41.0/39.1	44.4/42.6	27.0/26.3	35.3/33.9	40.1/38.8
ADHint (Ours)	64.8/64.3	49.5/50.6	60.4/59.1	51.4/50.0	33.3/32.0	42.6/41.4	50.3/49.6
<i>Base MLLM: Qwen2.5-VL-7B</i>							
SFT	59.0/68.7	40.1/ <u>64.0</u>	44.1/70.1	31.2/51.0	20.6/35.6	23.7/46.0	36.5/55.9
SFT → RL	64.7/71.1	<u>56.4</u> / 67.2	54.1/ 72.5	35.9/54.2	25.8/38.3	28.8/ <u>47.8</u>	44.3/ <u>58.5</u>
GRPO [33]	<u>73.4</u> / <u>73.4</u>	55.3/59.2	<u>69.8</u> /68.8	<u>55.3</u> / <u>55.6</u>	<u>40.4</u> / <u>40.0</u>	<u>44.9</u> /46.4	<u>56.5</u> /57.2
LUFFY [46]	63.6/61.2	34.6/38.1	52.2/54.8	44.6/47.4	30.6/29.7	40.2/39.2	44.3/45.1
StepHint [54]	47.2/49.5	27.7/31.4	39.8/41.1	18.6/27.9	9.5/19.3	10.5/22.7	25.6/32.0
HintGRPO [12]	65.9/64.3	45.9/47.5	42.9/44.7	40.6/39.3	30.2/28.7	36.4/34.7	43.7/43.2
GHPO [25]	66.1/63.9	52.3/48.9	63.0/52.8	51.7/50.0	35.3/32.3	42.4/40.5	51.8/48.1
ADHint (Ours)	74.4/74.8	60.6/61.8	69.9/70.8	56.4/56.4	41.3/41.8	48.7/49.4	58.6/59.2

Table 2: Math reasoning performance on Qwen2.5-Math-7B. We report *avg@32* on AIME and *pass@1* on all other benchmarks. †Results are taken from GHPO [25].

Method	AIME	AMC	Minerva	Math	Olympiad	Avg.
GRPO† [33]	27.0	62.5	34.6	81.0	44.8	50.0
LUFFY [46]	31.1	67.5	37.9	81.8	44.0	52.5
StepHint [54]	29.6	61.4	36.4	81.0	40.4	49.8
HintGRPO [12]	<u>32.8</u>	<u>71.1</u>	35.3	<u>83.0</u>	44.7	53.4
GHPO† [25]	32.0	70.0	<u>38.2</u>	82.2	<u>45.3</u>	<u>53.5</u>
ADHint (Ours)	33.6	72.3	41.5	84.6	47.3	55.9

Table 3: Medical VQA performance on PMC-Test using Qwen2.5-VL-7B.

Method	PMC-Test [56]
GRPO [33]	53.4
LUFFY [46]	49.4
StepHint [54]	48.3
HintGRPO [12]	20.9
GHPO [25]	52.9
ADHint (Ours)	55.1

hint-based methods, it delivers larger gains of 6.8%/11.1% (7B) and 9.7%/10.5% (3B). Furthermore, for Qwen3-VL models, ADHint maintains substantial effectiveness, boosting *pass@1*/*avg@8* by 5.1%/0.8% at 8B and 4.1%/3.0% at 4B over the baselines. Beyond the Qwen series, ADHint also achieves a 2.0%/2.2% improvement over the baselines on MiMo-VL-7B-SFT-2508. We observe that several baselines perform worse than vanilla GRPO, which is consistent with our motivation and the training dynamics observed. Methods that use fixed, high hint ratios (e.g., GHPO, HintGRPO) can introduce excessive guidance and yield extremely high training rewards (often > 0.9), but tend to overfit to the hint distribution, resulting in limited generalization and can even degrade reasoning ability without hints. Additionally, several methods (e.g., StepHint, LUFFY)

Table 4: Comparative performance on Qwen3-VL models. For each benchmark, we report *pass@1* (the first value) and *avg@8* (the second value).

Method	MathVista	MathVerse	We-Math	MMMU	MMMU-Pro	LogicVista	Avg.
<i>Base MLLM: Qwen3-VL-4B</i>							
GRPO [33]	73.6/77.9	56.1/75.9	67.9/82.1	38.1/49.5	39.4/51.2	46.2/60.8	53.6/66.2
LUFFY [46]	64.7/72.3	56.3/70.9	56.6/74.5	29.9/46.6	32.0/49.7	38.2/57.1	46.3/61.9
StepHint [54]	66.2/71.2	53.7/70.2	58.2/74.0	34.7/52.5	32.8/49.4	38.0/57.0	47.3/62.4
HintGRPO [12]	67.1/71.9	<u>60.3/72.8</u>	64.6/77.6	<u>42.0/52.2</u>	<u>40.1/49.4</u>	48.0/57.2	53.7/63.5
GHPO [25]	70.4/75.9	54.9/70.5	69.5/76.4	41.2/48.5	39.8/51.1	<u>48.4/59.0</u>	<u>54.0/63.6</u>
ADHint (Ours)	<u>71.7/77.6</u>	63.3/76.1	<u>69.3/81.0</u>	50.3/65.6	43.2/52.3	50.6/62.4	58.1/69.2
<i>Base MLLM: Qwen3-VL-8B</i>							
GRPO [33]	74.6/78.8	63.1/79.0	<u>73.1/82.6</u>	<u>61.0/71.7</u>	46.5/57.9	<u>49.4/63.0</u>	<u>61.3/72.2</u>
LUFFY [46]	54.4/53.7	28.0/18.6	26.0/18.1	21.0/26.6	21.2/27.2	14.5/21.8	27.5/27.7
StepHint [54]	55.0/54.8	28.4/20.5	25.8/17.5	22.5/27.7	22.3/27.2	20.5/22.5	29.1/28.4
HintGRPO [12]	64.9/64.4	<u>64.2/68.7</u>	68.6/71.7	47.2/55.5	38.4/46.0	43.1/51.9	54.4/59.7
GHPO [25]	64.9/63.2	39.7/37.7	49.9/48.8	38.8/38.5	40.4/40.0	45.1/43.6	46.5/45.3
ADHint (Ours)	<u>74.0/79.6</u>	75.2/80.1	76.4/85.6	<u>64.4/70.1</u>	51.8/57.9	56.3/64.9	66.4/73.0

Table 5: Comparative performance on MiMo-VL-7B-SFT-2508.

Method	MathVista	MathVerse	We-Math	MMMU	MMMU-Pro	LogicVista	Avg.
GRPO [33]	76.8/77.6	75.9/77.3	78.6/79.7	<u>64.5/65.9</u>	50.6/51.2	63.5/60.0	68.3/68.6
LUFFY [46]	70.2/68.1	64.5/68.7	60.7/67.5	48.2/61.4	35.2/47.4	41.7/53.7	53.4/61.1
StepHint [54]	72.3/67.9	64.5/67.8	63.2/66.6	36.2/43.3	37.0/47.2	43.3/54.6	52.8/57.9
HintGRPO [12]	80.4/79.0	79.0/77.8	<u>81.4/79.9</u>	57.6/56.6	<u>53.0/52.1</u>	59.7/60.5	68.5/67.7
GHPO [25]	78.8/76.4	72.7/61.7	78.7/74.6	63.7/60.4	50.8/46.6	<u>61.8/56.4</u>	67.8/62.7
ADHint (Ours)	<u>79.5/79.6</u>	<u>77.8/78.1</u>	81.6/81.6	68.3/68.7	53.7/54.1	<u>61.8/62.4</u>	70.5/70.8

ignore the imbalance in intra-group advantage estimation and the sharp gradients induced by hint tokens, leading to unstable update signals and training collapse. Moreover, our ViRL-Hint17k is more challenging, featuring longer reasoning chains (3100 tokens on average) than the relatively short baselines’ data (typically a few hundred tokens, e.g., ~ 230 in GHPO), which further exposes these shortcomings. To address these issues, ADHint introduces novel mechanisms for hint-ratio schedule, relative-advantage estimation, and hint gradient modulation, providing a feasible solution for hint-based on-policy learning on challenging multimodal tasks. A more in-depth comparative analysis of ADHint and the baselines is provided in Appendix E.

Performance with LLM. Table 2 evaluates ADHint on text-only reasoning. ADHint improves average accuracy by 2.4% over baselines across math reasoning benchmarks, indicating that it can broaden model capability boundaries across different modalities. Notably, the gains are consistent across benchmarks of varying difficulty, suggesting that ADHint benefits both routine and harder reasoning problems.

Generalization to different domains. Table 3 reports results on the Medical VQA domain, which is knowledge-intensive, more OOD for the backbone models, and

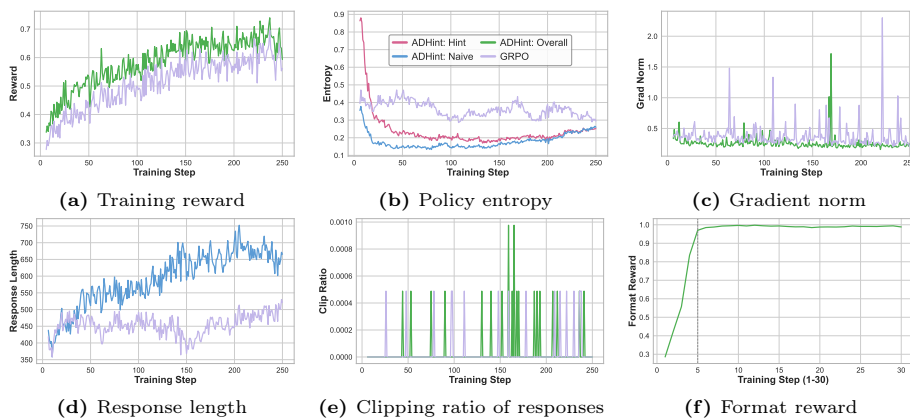


Fig. 5: Training dynamics of key metrics for ADHint and GRPO. “ADHint: Hint/Naive” reports metrics computed on hint- or naive-rollouts only, while “ADHint: Overall” aggregates both rollout types. ADHint maintains stable learning and yields concurrent improvements in reasoning generalization and knowledge expansion.

substantially different from standard math reasoning. We observe that the baselines do not generalize well, whereas ADHint improves accuracy by 1.7% over GRPO. These results suggest that ADHint can be readily transferred to more challenging real-world domains.

5.3 Training Dynamics

Figure 5 presents the training dynamics of several key metrics. Figure 5a shows that ADHint consistently maintains rewards within a moderate regime, yielding low-variance update signals. Figures 5b and 5c indicate that ADHint maintains exploration within a healthy entropy range with more stable gradient updates. Figures 5d and 5e show that ADHint steadily increases response length, while the proportion of overlength responses does not increase, which usually indicates repetition or garbled outputs. These trends suggest that the policy model continuously acquires effective long-term thinking capabilities. Taken together, these observations indicate that ADHint stably and adaptively learns reasoning ability from off-policy hints.

5.4 Ablation Study

Table 6 reports the ablation results of four critical components in ADHint. Specifically, “w/o AH-SDP” replaces our adaptive hint-ratio schedule with an annealing hint-ratio strategy, while “w/o AE-RDP” pools hint-rollouts and naive-rollouts into a single group for advantage estimation. Removing any component results in performance degradation on both *pass@1* and *avg@8*, underscoring the importance of our design. The difficulty-aware design in the hint-ratio schedule

Table 6: Ablation study of proposed ADHint. For each benchmark, we report *pass@1* (the first value) and *avg@8* (the second value).

Method	MathVista	MathVerse	We-Math	MMMU	MMMU-Pro	LogicVista	Avg.
ADHint	74.4/74.8	60.6/61.8	69.9/70.8	56.4/56.4	41.3/41.8	48.7/49.4	58.6/59.2
w/o AH-SDP	74.1/73.5	58.7/58.9	68.6/67.4	54.6/55.0	41.3/40.3	48.2/48.4	57.6/57.3
w/o AE-RDP	74.3/74.1	61.5/60.0	67.5/68.4	55.9/56.1	41.2/41.1	45.8/46.3	57.7/57.7
w/o CGM	73.1/72.8	53.9/55.0	68.2/68.0	56.3/51.1	40.0/40.0	50.5/48.2	57.0/55.9
w/o Selective Masking	74.7/73.7	58.5/61.0	67.4/67.6	55.8/55.9	41.6/40.9	47.3/46.3	57.6/57.6

Table 7: Effect of the maximum hint ratio w_{\max} .

Setting	MathVista	MathVerse	We-Math	MMMU	MMMU-Pro	LogicVista	Avg.
$w_{\max} = 0$	73.4/73.4	55.3/59.2	69.8/68.8	55.3/55.6	40.4/40.0	44.9/46.4	56.5/57.2
$w_{\max} = 0.2$	74.4/74.8	60.6/61.8	69.9/70.8	56.4/56.4	41.3/41.8	48.7/49.4	58.6/59.2
$w_{\max} = 0.4$	73.8/73.5	62.6/57.9	68.2/67.5	54.8/54.5	41.3/40.1	47.3/47.5	58.0/56.8
$w_{\max} = 0.6$	73.8/72.4	56.9/59.7	65.5/67.7	54.9/55.5	39.3/40.2	46.9/47.5	56.2/57.2

Table 8: Effect of the threshold α in CGM.

Setting	MathVista	MathVerse	We-Math	MMMU	MMMU-Pro	LogicVista	Avg.
$\alpha = 0.25$	72.0/72.8	56.0/59.5	67.9/68.6	55.3/55.6	40.9/40.7	48.9/48.1	56.8/57.6
$\alpha = 0.5$	74.4/74.8	60.6/61.8	69.9/70.8	56.4/56.4	41.3/41.8	48.7/49.4	58.6/59.2
$\alpha = 0.75$	76.0/75.1	53.4/ 62.8	66.3/68.6	55.2/56.3	40.3/41.2	47.5/47.4	56.5/58.6

and relative-advantage estimation ensures efficient learning that balances exploration and imitation. The gradient modulation mechanisms prevent biased and destructive updates, ensuring healthy policy learning.

5.5 Further Analysis

20% hint is sufficient to guide reasoning. In Table 7, we vary w_{\max} and observe that performance is optimal when it is set to 0.2. Both increasing and decreasing the hint ratio lead to performance degradation. As shown in Figure 5a, a 20% hint ratio is sufficient to keep rewards within the range of 0.5–0.7, providing stable learning signals at a moderate difficulty level. Further increasing the hint ratio yields excessively high rewards for hint-rollouts, which introduces larger update bias. These results suggest that the initial prefix of the reasoning trajectory is critical for steering the policy model toward effective reasoning.

Hint-token gradients should be restricted to a reasonable range. In Table 8, we investigate the CGM threshold α , which controls the gradient contributions of hint tokens. The results indicate that setting α to 0.5 yields the best overall performance. Allowing hint tokens with excessively high or low entropy to participate in gradient updates causes the policy to deviate markedly from its initial distribution. In contrast, an overly small threshold limits effective learning from off-policy hints and reduces the efficiency of knowledge expansion.

6 Conclusion

In this work, we propose **ADHint**, which explicitly incorporates difficulty into hint-based on-policy learning. Enhanced by critical components that schedule the hint ratio with respect to the sample difficulty prior, estimate relative advantages with respect to the rollout difficulty posterior, and modulate token-level gradients based on distribution consistency, ADHint surpasses existing methods across diverse settings, showcasing advanced reasoning abilities and OOD generalization. Despite its impressive performance, ADHint’s scaling behavior on larger models with 32B or more parameters, as well as its generalization to tasks without verifiable answers, merits further investigation.

References

1. Bai, S., Cai, Y., Chen, R., Chen, K., Chen, X., Cheng, Z., Deng, L., Ding, W., Gao, C., Ge, C., Ge, W., Guo, Z., Huang, Q., Huang, J., Huang, F., Hui, B., Jiang, S., Li, Z., Li, M., Li, M., Li, K., Lin, Z., Lin, J., Liu, X., Liu, J., Liu, C., Liu, Y., Liu, D., Liu, S., Lu, D., Luo, R., Lv, C., Men, R., Meng, L., Ren, X., Ren, X., Song, S., Sun, Y., Tang, J., Tu, J., Wan, J., Wang, P., Wang, P., Wang, Q., Wang, Y., Xie, T., Xu, Y., Xu, H., Xu, J., Yang, Z., Yang, M., Yang, J., Yang, A., Yu, B., Zhang, F., Zhang, H., Zhang, X., Zheng, B., Zhong, H., Zhou, J., Zhou, F., Zhou, J., Zhu, Y., Zhu, K.: Qwen3-vl technical report (2025), <https://arxiv.org/abs/2511.21631>
2. Bai, S., Chen, K., Liu, X., Wang, J., Ge, W., Song, S., Dang, K., Wang, P., Wang, S., Tang, J., et al.: Qwen2.5-vl technical report. arXiv preprint arXiv:2502.13923 (2025)
3. Bengio, Y., Louradour, J., Collobert, R., Weston, J.: Curriculum learning. In: Proceedings of the 26th annual international conference on machine learning. pp. 41–48 (2009)
4. Chen, X., Liao, M., Chen, G., Li, C., Fu, B., Fan, K., Liu, X.: From data-centric to sample-centric: Enhancing llm reasoning via progressive optimization. arXiv preprint arXiv:2507.06573 (2025)
5. Chu, T., Zhai, Y., Yang, J., Tong, S., Xie, S., Schuurmans, D., Le, Q.V., Levine, S., Ma, Y.: Sft memorizes, rl generalizes: A comparative study of foundation model post-training. In: Forty-second International Conference on Machine Learning (2025)
6. Dong, Y., Jiang, X., Tao, Y., Liu, H., Zhang, K., Mou, L., Cao, R., Ma, Y., Chen, J., Li, B., et al.: RL-plus: Countering capability boundary collapse of llms in reinforcement learning with hybrid-policy optimization. arXiv preprint arXiv:2508.00222 (2025)
7. Fu, Y., Chen, T., Chai, J., Wang, X., Tu, S., Yin, G., Lin, W., Zhang, Q., Zhu, Y., Zhao, D.: Srft: A single-stage method with supervised and reinforcement fine-tuning for reasoning. arXiv preprint arXiv:2506.19767 (2025)
8. Guo, D., Yang, D., Zhang, H., Song, J., Wang, P., Zhu, Q., Xu, R., Zhang, R., Ma, S., Bi, X., et al.: Deepseek-r1 incentivizes reasoning in llms through reinforcement learning. *Nature* **645**(8081), 633–638 (2025)
9. He, C., Luo, R., Bai, Y., Hu, S., Thai, Z.L., Shen, J., Hu, J., Han, X., Huang, Y., Zhang, Y., et al.: Olympiadbench: A challenging benchmark for promoting agi with olympiad-level bilingual multimodal scientific problems. arXiv preprint arXiv:2402.14008 (2024)

10. Hendrycks, D., Burns, C., Kadavath, S., Arora, A., Basart, S., Tang, E., Song, D., Steinhardt, J.: Measuring mathematical problem solving with the math dataset. In: *Thirty-fifth Conference on Neural Information Processing Systems Datasets and Benchmarks Track (Round 2)* (2021)
11. Hendrycks, D., Burns, C., Kadavath, S., Arora, A., Basart, S., Tang, E., Song, D., Steinhardt, J.: Measuring mathematical problem solving with the math dataset. *NeurIPS* (2021)
12. Huang, Q., Dai, W., Liu, J., He, W., Jiang, H., Song, M., Chen, J., Yao, C., Song, J.: Boosting mllm reasoning with text-debiased hint-grpo. In: *Proceedings of the IEEE/CVF International Conference on Computer Vision (ICCV)*. pp. 4848–4857 (October 2025)
13. Huang, W., Jia, B., Zhai, Z., Cao, S., Ye, Z., Zhao, F., Xu, Z., Hu, Y., Lin, S.: Vision-r1: Incentivizing reasoning capability in multimodal large language models. *arXiv preprint arXiv:2503.06749* (2025)
14. Huang, Z., Cheng, T., Qiu, Z., Wang, Z., Xu, Y., Ponti, E.M., Titov, I.: Blending supervised and reinforcement fine-tuning with prefix sampling. *arXiv preprint arXiv:2507.01679* (2025)
15. Lewkowycz, A., Andreassen, A., Dohan, D., Dyer, E., Michalewski, H., Ramasesh, V., Slone, A., Anil, C., Schlag, I., Gutman-Solo, T., et al.: Solving quantitative reasoning problems with language models. *Advances in neural information processing systems* **35**, 3843–3857 (2022)
16. Li, J., Beeching, E., Tunstall, L., Lipkin, B., Soletskyi, R., Huang, S., Rasul, K., Yu, L., Jiang, A.Q., Shen, Z., et al.: Numinamath: The largest public dataset in ai4maths with 860k pairs of competition math problems and solutions. *Hugging Face repository* **13**(9), 9 (2024)
17. Li, R., Huang, H., Wei, F., Xiong, F., Wang, Y., Chu, X.: Adacurl: Adaptive curriculum reinforcement learning with invalid sample mitigation and historical revisiting. *arXiv preprint arXiv:2511.09478* (2025)
18. Li, S., Deng, K., Wang, L., Yang, H., Peng, C., Yan, P., Shen, F., Shen, H.T., Xu, X.: Truth in the few: High-value data selection for efficient multi-modal reasoning. *arXiv preprint arXiv:2506.04755* (2025)
19. Li, Z.Z., Zhang, D., Zhang, M.L., Zhang, J., Liu, Z., Yao, Y., Xu, H., Zheng, J., Wang, P.J., Chen, X., et al.: From system 1 to system 2: A survey of reasoning large language models. *arXiv preprint arXiv:2502.17419* (2025)
20. Li, Z., Sun, Z., Zhao, J., Min, E., Zeng, Y., Wu, H., Cai, H., Wang, S., Yin, D., Chen, X., et al.: Staying in the sweet spot: Responsive reasoning evolution via capability-adaptive hint scaffolding. *arXiv preprint arXiv:2509.06923* (2025)
21. Liang, Y., Qiu, J., Ding, W., Liu, Z., Tompkin, J., Xu, M., Xia, M., Tu, Z., Shi, L., Zhu, J.: Modomodo: Multi-domain data mixtures for multimodal llm reinforcement learning (2025), <https://arxiv.org/abs/2505.24871>
22. Liu, M., Farina, G., Ozdaglar, A.E.: UFT: Unifying supervised and reinforcement fine-tuning. In: *The Thirty-ninth Annual Conference on Neural Information Processing Systems* (2025), <https://openreview.net/forum?id=us0kGv1S7M>
23. Liu, X., Ni, J., Wu, Z., Du, C., Dou, L., Wang, H., Pang, T., Shieh, M.Q.: Noisyrollout: Reinforcing visual reasoning with data augmentation. *arXiv preprint arXiv:2504.13055* (2025)
24. Liu, Y., Qu, T., Zhong, Z., Peng, B., Liu, S., Yu, B., Jia, J.: Visionreasoner: Unified visual perception and reasoning via reinforcement learning. *arXiv preprint arXiv:2505.12081* (2025)

25. Liu, Z., Gong, C., Fu, X., Liu, Y., Chen, R., Hu, S., Zhang, S., Liu, R., Zhang, Q., Tu, D.: Ghpo: Adaptive guidance for stable and efficient llm reinforcement learning. arXiv preprint arXiv:2507.10628 (2025)
26. Liu, Z., Sun, Z., Zang, Y., Dong, X., Cao, Y., Duan, H., Lin, D., Wang, J.: Visual-rlft: Visual reinforcement fine-tuning. arXiv preprint arXiv:2503.01785 (2025)
27. Lu, P., Bansal, H., Xia, T., Liu, J., Li, C., Hajishirzi, H., Cheng, H., Chang, K.W., Galley, M., Gao, J.: Mathvista: Evaluating math reasoning in visual contexts with gpt-4v, bard, and other large multimodal models. CoRR (2023)
28. Ma, L., Liang, H., Qiang, M., Tang, L., Ma, X., Wong, Z.H., Niu, J., Shen, C., He, R., Li, Y., et al.: Learning what reinforcement learning can't: Interleaved online fine-tuning for hardest questions. arXiv preprint arXiv:2506.07527 (2025)
29. Parashar, S., Gui, S., Li, X., Ling, H., Vemuri, S., Olson, B., Li, E., Zhang, Y., Caverlee, J., Kalathil, D., et al.: Curriculum reinforcement learning from easy to hard tasks improves llm reasoning. arXiv preprint arXiv:2506.06632 (2025)
30. Patel, B., Chakraborty, S., Suttle, W.A., Wang, M., Bedi, A.S., Manocha, D.: Aime: Ai system optimization via multiple llm evaluators. arXiv preprint arXiv:2410.03131 (2024)
31. Qiao, R., Tan, Q., Dong, G., Wu, M., Sun, C., Song, X., GongQue, Z., Lei, S., Wei, Z., Zhang, M., et al.: We-math: Does your large multimodal model achieve human-like mathematical reasoning? arXiv preprint arXiv:2407.01284 (2024)
32. Schulman, J., Wolski, F., Dhariwal, P., Radford, A., Klimov, O.: Proximal policy optimization algorithms. arXiv preprint arXiv:1707.06347 (2017)
33. Shao, Z., Wang, P., Zhu, Q., Xu, R., Song, J., Bi, X., Zhang, H., Zhang, M., Li, Y., et al.: Deepseekmath: Pushing the limits of mathematical reasoning in open language models. arXiv preprint arXiv:2402.03300 (2024)
34. Su, A., Wang, H., Ren, W., Lin, F., Chen, W.: Pixel reasoner: Incentivizing pixel-space reasoning with curiosity-driven reinforcement learning. arXiv preprint arXiv:2505.15966 (2025)
35. Tan, Z., Gao, H., Ma, X., Zhang, F., Dong, Z.: Towards flash thinking via decoupled advantage policy optimization. arXiv preprint arXiv:2510.15374 (2025)
36. Team, K., Bai, Y., Bao, Y., Chen, G., Chen, J., Chen, N., Chen, R., Chen, Y., Chen, Y., Chen, Y., et al.: Kimi k2: Open agentic intelligence. arXiv preprint arXiv:2507.20534 (2025)
37. Team, M.L., Li, B., Lei, B., Wang, B., Rong, B., Wang, C., Zhang, C., Gao, C., Zhang, C., Sun, C., et al.: Longcat-flash technical report. arXiv preprint arXiv:2509.01322 (2025)
38. Wang, H., Qu, C., Huang, Z., Chu, W., Lin, F., Chen, W.: Vl-rethinker: Incentivizing self-reflection of vision-language models with reinforcement learning. arXiv preprint arXiv:2504.08837 (2025)
39. Wang, W., Gao, Z., Gu, L., Pu, H., Cui, L., Wei, X., Liu, Z., Jing, L., Ye, S., Shao, J., et al.: Internvl3. 5: Advancing open-source multimodal models in versatility, reasoning, and efficiency. arXiv preprint arXiv:2508.18265 (2025)
40. Wang, Y., Yang, Q., Zeng, Z., Ren, L., Liu, L., Peng, B., Cheng, H., He, X., Wang, K., Gao, J., et al.: Reinforcement learning for reasoning in large language models with one training example. arXiv preprint arXiv:2504.20571 (2025)
41. Wang, Z., Guo, X., Stoica, S., Xu, H., Wang, H., Ha, H., Chen, X., Chen, Y., Yan, M., Huang, F., et al.: Perception-aware policy optimization for multimodal reasoning. arXiv preprint arXiv:2507.06448 (2025)
42. Wu, J., Liao, C., Feng, M., Zhang, S., Wen, Z., Luo, H., Yang, L., Xu, H., Tao, J.: Templaterl: Structured template-guided reinforcement learning for llm reasoning (2025), <https://arxiv.org/abs/2505.15692>

43. Xi, Z., Guo, X., Nan, Y., Zhou, E., Shen, J., Chen, W., Liu, J., Huang, J., Zhang, Z., Guo, H., Deng, X., Lei, Z., Zheng, M., Wang, G., Zhang, S., Sun, P., Zheng, R., Yan, H., Gui, T., Zhang, Q., Huang, X.: Bapo: Stabilizing off-policy reinforcement learning for llms via balanced policy optimization with adaptive clipping (2025), <https://arxiv.org/abs/2510.18927>
44. Xiao, Y., Sun, E., Liu, T., Wang, W.: Logicvista: Multimodal llm logical reasoning benchmark in visual contexts. arXiv preprint arXiv:2407.04973 (2024)
45. Xiaomi, L.C.T.: Mimo-vl technical report (2025), <https://arxiv.org/abs/2506.03569>
46. Yan, J., Li, Y., Hu, Z., Wang, Z., Cui, G., Qu, X., Cheng, Y., Zhang, Y.: Learning to reason under off-policy guidance. In: The Thirty-ninth Annual Conference on Neural Information Processing Systems (2025), <https://openreview.net/forum?id=v08LLoNWWk>
47. Yang, A., Li, A., Yang, B., Zhang, B., Hui, B., Zheng, B., Yu, B., Gao, C., Huang, C., Lv, C., et al.: Qwen3 technical report. arXiv preprint arXiv:2505.09388 (2025)
48. Yang, A., Zhang, B., Hui, B., Gao, B., Yu, B., Li, C., Liu, D., Tu, J., Zhou, J., Lin, J., et al.: Qwen2.5-math technical report: Toward mathematical expert model via self-improvement. arXiv preprint arXiv:2409.12122 (2024)
49. Ye, Y., Huang, Z., Xiao, Y., Chern, E., Xia, S., Liu, P.: Limo: Less is more for reasoning. arXiv preprint arXiv:2502.03387 (2025)
50. Yu, Q., Zhang, Z., Zhu, R., Yuan, Y., Zuo, X., Yue, Y., Dai, W., Fan, T., Liu, G., Liu, L., et al.: Dapo: An open-source llm reinforcement learning system at scale. arXiv preprint arXiv:2503.14476 (2025)
51. Yue, X., Ni, Y., Zhang, K., Zheng, T., Liu, R., Zhang, G., Stevens, S., Jiang, D., Ren, W., Sun, Y., et al.: Mmmu: A massive multi-discipline multimodal understanding and reasoning benchmark for expert agi. In: Proceedings of the IEEE/CVF Conference on Computer Vision and Pattern Recognition. pp. 9556–9567 (2024)
52. Yue, X., Zheng, T., Ni, Y., Wang, Y., Zhang, K., Tong, S., Sun, Y., Yu, B., Zhang, G., Sun, H., et al.: Mmmu-pro: A more robust multi-discipline multimodal understanding benchmark. arXiv preprint arXiv:2409.02813 (2024)
53. Zeng, A., Lv, X., Zheng, Q., Hou, Z., Chen, B., Xie, C., Wang, C., Yin, D., Zeng, H., Zhang, J., et al.: Glm-4.5: Agentic, reasoning, and coding (arc) foundation models. arXiv preprint arXiv:2508.06471 (2025)
54. Zhang, K., Lv, A., Li, J., Wang, Y., Wang, F., Hu, H., Yan, R.: Stephint: Multi-level stepwise hints enhance reinforcement learning to reason. arXiv preprint arXiv:2507.02841 (2025)
55. Zhang, R., Jiang, D., Zhang, Y., Lin, H., Guo, Z., Qiu, P., Zhou, A., Lu, P., Chang, K.W., Qiao, Y., et al.: Mathverse: Does your multi-modal llm truly see the diagrams in visual math problems? In: European Conference on Computer Vision. pp. 169–186. Springer (2024)
56. Zhang, X., Wu, C., Zhao, Z., Lin, W., Zhang, Y., Wang, Y., Xie, W.: Pmc-vqa: Visual instruction tuning for medical visual question answering. arXiv preprint arXiv:2305.10415 (2023)
57. Zhang, X., Huang, Z., Li, Y., Ni, C., Chen, J., Oymak, S.: Bread: Branched rollouts from expert anchors bridge sft & rl for reasoning. arXiv preprint arXiv:2506.17211 (2025)
58. Zheng, Y., Lu, J., Wang, S., Feng, Z., Kuang, D., Xiong, Y.: Easyrl: An efficient, scalable, multi-modality rl training framework. <https://github.com/hiyouga/EasyR1> (2025)

59. Zheng, Z., Yang, M., Hong, J., Zhao, C., Xu, G., Yang, L., Shen, C., Yu, X.: Deepeyes: Incentivizing “thinking with images” via reinforcement learning. arXiv preprint arXiv:2505.14362 (2025)
60. Zhu, W., Dong, X., Li, X., Qiu, P., Chen, X., Razi, A., Sotiras, A., Su, Y., Wang, Y.: Toward effective reinforcement learning fine-tuning for medical vqa in vision-language models. arXiv preprint arXiv:2505.13973 (2025)

A Overview

Our appendix is organized as follows:

- **Section B** presents the detailed workflow of ADHint.
- **Section C** provides an extended discussion of related work.
- **Section D** offers additional details on training data construction, experimental settings, and the reimplementations of baselines.
- **Section E** conducts an in-depth comparison between ADHint and the baselines, analyzing the sources of their performance differences.
- **Section F** provides several case studies to offer a more intuitive view of ADHint’s behavior.

B Training Algorithm of ADHint

In Algorithm 1, we provide the detailed workflow of ADHint as a complement to the main text.

Algorithm 1 ADHint: ADaptive Hints with Difficulty Priors for Reinforcement Learning

Require: Initial policy model π_θ , training set \mathcal{D} , hyperparameters $w_{\max}, w_{\min}, \alpha$

Ensure: Optimized policy model π_θ^*

```

for step = 1, ..., S do
  Sample a mini-batch  $\mathcal{D}_b \subset \mathcal{D}$ 
  for each  $q \in \mathcal{D}_b$  do
    Generate naive-rollouts  $o_{1:n} \sim \pi_\theta(\cdot | q)$ 
    Compute  $\text{Diff}_N$  by Eq. 1
    Compute hint ratio  $w$  by Eq. 2
    Generate hint-rollouts  $o_{n+1:n+m} \sim \pi_\theta(\cdot | q, o_{i,<h})$ 
    Compute  $\text{Diff}_H$  by Eq. 6
    Compute relative advantages  $\tilde{A}_i$  by Eq. 7
    for each hint-rollout  $o_i \in \{o_{n+1}, \dots, o_{n+m}\}$  do
      Compute token entropy by Eq. 3
      Compute continuation entropy by Eq. 4
      Compute token-wise gradient modulation factors  $k_{i,t}$  by Eq. 5
    end for
  end for
  Update  $\theta$  by ascending  $\mathcal{J}_{\text{ADHint}}^*(\pi_\theta)$  in Eq. 8
end for
return  $\pi_\theta^*$ 

```

C Detailed Related Work

Multimodal Reinforcement Learning GRPO [8, 33] removes the critic network from PPO [32] and estimates advantages through intra-group sampling. This

approach has become a cornerstone for the development of recent reasoning models [35–37, 40, 47, 49, 53]. In parallel, the multimodal community has explored various strategies to enhance the reasoning ability of MLLMs. Some works refine the reasoning style by encouraging models to “think with images” [34, 59], explicitly grounding reasoning in visual features and directing attention to specific objects or regions. VL-ReThinker [38] introduces an explicit reflection phase into the reasoning process, allowing the model to revisit and revise its initial thoughts. Other methods inject noise into rollouts [23, 41] to improve training robustness and mitigate hallucinations. There are also approaches that design more precise reward functions for tasks such as object detection and semantic segmentation [24, 26], as well as methods that select or curate training data to improve efficiency [18, 21]. However, these advances primarily unlock the latent potential of pretrained models, often failing to expand their fundamental capability boundaries.

Reinforcement Learning with Off-Policy Hints Recent work has investigated how to incorporate off-policy data into RL-based post-training. Some approaches directly integrate off-policy data into the SFT or RL objective [6, 7, 28, 46], but they struggle with the substantial distribution mismatch between off-policy data and the current policy model. To alleviate this issue, some methods design corrections for importance sampling [6, 46], control the trade-off between SFT and RL losses via entropy-based schedules [7], or alternate between RL and SFT phases [28]. Hint-based methods address this problem more flexibly by guiding the model’s reasoning with partial hints extracted from off-policy data while preserving its exploration behavior. UFT [22] and Prefix-RFT [14] employ the same temporally annealed hint ratios for all samples. SEELE [20] introduces learnable parameters to predict instance-specific hint ratios in a multi-round training scheme. Other methods reserve hints only for the hardest samples and determine the hint ratio from a fixed, predefined set via uniform sampling [4], binary search [57], or progressive search [12, 25]. StepHint [54] samples rollouts under multiple hint ratios and merges the resulting hint-rollouts, naive-rollouts, and ground truth off-policy data into a single group for advantage estimation. However, these methods often overlook difficulty as a key factor, leading to insufficient and unstable training. In this work, we propose ADHint, which explicitly incorporates the sample difficulty prior into the hint-ratio schedule and the rollout difficulty posterior into relative-advantage estimation. This difficulty-aware design stabilizes training, enhances exploration, and expands the model’s knowledge boundary when learning from off-policy hints.

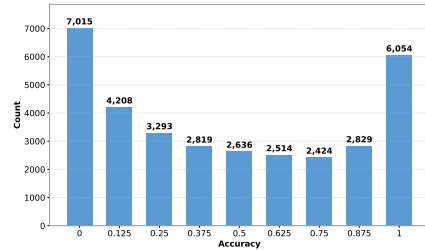
D Detailed Experimental Settings

D.1 Training data

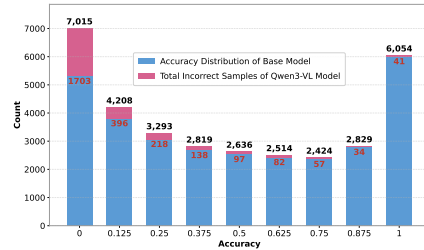
For MLLM training, we construct an off-policy hint dataset based on ViRL39K [38], which covers STEM, chart reasoning, document reasoning, and spatial reasoning.

We first remove samples that involve multi-image reasoning, text-only reasoning, or format errors, obtaining roughly 34K examples. Figure 6a shows the $avg@8$ distribution of Qwen2.5-VL-7B on this filtered set. We then sample hints with Qwen3-VL-30B-A3B-Thinking, and Figure 6b reports the distribution of examples for which this model fails to produce any correct hint among eight candidates. For these hard cases, we further sample hints with Qwen3-VL-235B-A22B-Thinking, whose $avg@8$ distribution is shown in Figure 6c. Among samples with at least one correct hint, we discard those with hint length exceeding 8K tokens and randomly select one of the eight candidates as the final hint, with the resulting hint-length distribution shown in Figure 6d. Finally, we remove samples that are excessively simple for Qwen2.5-VL-7B and obtain ViRL-Hint17k, which we will open-source.

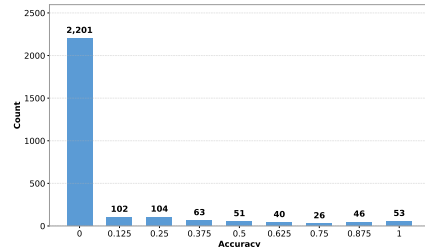
For Medical VQA, we similarly employ Qwen3-VL-30B-A3B-Thinking to sample hints from the PMC-VQA training set [56], ultimately constructing a filtered subset of 15K samples. For LLM training, we utilize NuminaMath-S curated by GHPO [25], which comprises 18.3K samples combined from MATH [10] and NuminaMath-1.5 [11].



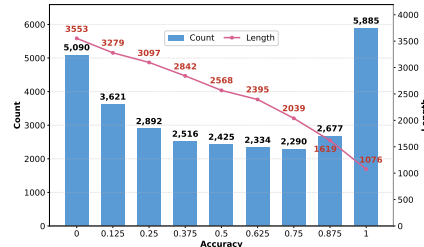
(a) $avg@8$ distribution of Qwen2.5-VL-7B (base model) on the 34K filtered samples.



(b) Distribution of samples for which Qwen3-VL-30B-A3B-Thinking fails to produce any correct hint among eight candidates.



(c) $avg@8$ distribution of Qwen3-VL-235B-A22B-Thinking on the remaining hard samples.



(d) Hint-length distribution and base model accuracy after hint sampling.

Fig. 6: Accuracy and length statistics during ViRL-Hint17k construction. At each sampling stage, we independently generate eight reasoning trajectories with temperature 1.0.

D.2 Benchmarks

For MLLM evaluation, we employ six benchmarks that cover mathematical reasoning, multidisciplinary multimodal reasoning, and logical reasoning:

- **MathVista** — A consolidated benchmark for mathematical reasoning in visual contexts, which unifies math-focused and vision–language tasks into a single suite and requires fine-grained visual understanding and compositional reasoning. We use the testmini split for evaluation.
- **MathVerse** — A holistic visual math benchmark that is crafted to test whether multimodal models truly understand mathematical diagrams, providing multiple variants of each problem with different modality configurations to probe robust diagram understanding. We use the Vision-Only subset.
- **We-Math** — A large-scale benchmark that investigates human-like mathematical reasoning in MLLMs, decomposing problems into sub-problems and introducing multi-dimensional metrics to analyze knowledge acquisition, generalization, and rote memorization behaviours. We use the testmini split.
- **MMMU** — A massive multi-discipline multimodal understanding benchmark that spans college-level subjects such as science, engineering, humanities, and business, and demands deliberate integration of visual and textual information for complex problem solving. We use the validation split.
- **MMMU-Pro** — A more challenging variant of MMMU that filters out text-only questions, augments candidate options, and introduces vision-only settings, thereby providing a more robust assessment of genuine multimodal understanding and reasoning. We use the standard subset with 10 options and the vision subset to compute the overall score.
- **LogicVista** — A benchmark that targets integrated logical reasoning in visual environments, focusing on compositional, step-by-step reasoning over diagrams and structured visual scenes.

For Medical VQA, we evaluate on the PMC-VQA test set, a comprehensive benchmark derived from PubMed Central that assesses a model’s ability to comprehend medical images and generate clinically grounded answers.

For LLM evaluation, we employ five mathematical reasoning benchmarks that align with our training domain:

- **AIME24** — A dataset that contains 30 competition-style problems from the 2024 American Invitational Mathematics Examination (AIME), a well-known high-school contest featuring challenging short-answer problems.
- **AMC** — A benchmark constructed from the American Mathematics Competitions, covering a broad range of high-school mathematics topics and providing multiple-choice questions that emphasize conceptual understanding and problem-solving skills.
- **MATH500** — A high-difficulty math competition benchmark containing 500 problems across multiple subjects, designed to assess advanced problem-solving and multi-step symbolic reasoning.

- **Minerva** — A quantitative reasoning benchmark with around 500 carefully curated math problems that require multi-step derivations and the integration of textual descriptions with formal mathematical manipulations.
- **OlympiadBench** — An Olympiad-level benchmark that comprises thousands of mathematically and scientifically challenging problems, offering a rigorous testbed for models’ higher-order reasoning and abstraction abilities.

D.3 Implementation Details

As a supplement to the main text, Tables 9 and 10 summarize the training configs of the GRPO and SFT baselines, respectively. Table 11 reports the default configs for ADHint, with the exception of MiMo-VL-7B-SFT-2508, Qwen2.5-Math-7B, and Medical VQA (based on Qwen2.5-VL-7B), where the maximum hint ratio w_{\max} is set to 0.4. Note that both GRPO and ADHint use 16 rollouts to ensure a fair comparison.

D.4 Baselines

We compare ADHint against a diverse set of baselines to validate its effectiveness. These include standard on-policy RL, supervised fine-tuning, and recent methods that attempt to incorporate off-policy data into on-policy RL training:

- **GRPO** — an on-policy RL method that estimates group-level relative advantages from rollouts and relies solely on an outcome reward function or model.
- **SFT** — a supervised baseline that directly trains the model to imitate complete off-policy trajectories (full hints in our setting), which encourages memorization of both knowledge and response style.
- **SFT** \rightarrow **RL** — a common cold-start strategy that first performs SFT and then applies RL, serving as a strong baseline that combines the benefits of SFT and RL.
- **LUFFY** — a method that augments GRPO by incorporating off-policy reasoning trajectories into the GRPO objective.
- **StepHint** — a hint-based method that mixes hint-rollouts under multiple hint ratios, naive-rollouts, and off-policy reasoning trajectories into a single GRPO group for advantage estimation.
- **HintGRPO** — a method that focuses on the hardest samples where the current policy fails to obtain a positive rollout. It progressively increases the hint ratio (1/3, 2/3) once a positive rollout is found, followed by a one-step policy update.
- **GHPO** — a method that treats hints as part of the query and excludes hint tokens from loss computation. It similarly increases the hint ratio (25%, 50%, 75%) once a positive rollout is found.

For methods that do not support MLLM training or whose code is not publicly available, we carefully reproduce them within the EasyR1 framework [58]. We note that several baselines exhibit instability and crash during training. We provide a detailed analysis in Section E.

Table 9: Training configs for GRPO baselines.

Model	Config	Value
Qwen2.5-VL & Qwen3-VL & MiMo-VL-SFT	max prompt length	4096
	max response length	8192
	temperature	1.0
	learning rate	1e-6
	rollout batchsize	128
	global batchsize	64
	num rollouts	16
	epoch	2
	min pixels	256 * 28 * 28
	max pixels	1280 * 28 * 28
Qwen2.5-Math	max prompt length	2048
	max response length	2048
	temperature	1.0
	learning rate	1e-6
	lr schedule	cosine
	warmup ratio	0.1
	rollout batchsize	128
	global batchsize	32
epoch	5	

Table 10: Training configs for SFT baselines.

Method	Config	Value
SFT	learning rate	5e-5
	lr schedule	cosine
	warmup ratio	0.1
	batchsize	64
	epoch	2
	min pixels	256 × 28 × 28
	max pixels	1280 × 28 × 28

Table 11: Training configs for ADHint.

Method	Config	Value
ADHint	warmup steps	5
	num of naive-rollouts n	8
	num of hint-rollouts m	8
	maximum hint ratio w_{\max}	0.2
	sampling radius of the noise term θ	0.01
	threshold of CGM α	0.5

D.5 Reimplementation Details of Baselines

For all baselines, we strictly follow the official implementations and the settings reported in the original papers. We train each method for 2 epochs on the same ViRL-Hint17k dataset to ensure a fair comparison. Below, we describe the reimplementation details for each baseline.

LUFFY. Following the paper, we add an off-policy objective to the standard GRPO objective to obtain the mixed-policy training. We also reimplement the policy shaping module to modulate the update gradients of off-policy tokens and set the shaping hyperparameter to the default value of 0.1 reported in LUFFY. We omit both the KL divergence constraint and the standard advantage normalization.

StepHint. We obtain hint-rollouts under hint ratios of 25%, 50%, and 75%, and group them with naive-rollouts and complete off-policy reasoning trajectories into a single GRPO group for relative advantage estimation. We omit the KL constraint and mask hint tokens during optimization for negative hint-rollouts.

HintGRPO. We set the group number to $M = 3$, so the hint ratio is progressively increased from 0 to $1/3$ and then $2/3$ until a positive rollout appears. We set the KL coefficient to 0.04 and the maximum response length to 8K tokens. This setting matches our ViRL-Hint17k dataset, which has a relatively long average hint length (around 3100 tokens) and is substantially longer than that in the original HintGRPO experiments. We do not reproduce the *Text-Bias Calibration* module from HintGRPO because it is a test-time method for correcting perception bias and mitigating hallucinations rather than a training-time hint-based component.

GHPO. For the hardest samples where the current policy fails to produce a correct answer, we insert hints into the user prompt using the official prompt template. The hint ratio is progressively increased from 25% to 50% and then to 75% until a positive rollout appears. We then use the corresponding hint-rollouts as the update signal for that sample. Following the original paper, we omit the KL constraint and apply a 5-step GRPO warmup.

E Comparative Analysis of ADHint and Baselines

As shown in Figure 2, ADHint consistently outperforms all baselines. Here, we provide a detailed comparative analysis of ADHint and these baselines to better understand the sources of their performance differences.

SFT learns, RL generalizes. As shown in Table 1, compared with pure GRPO, the SFT \rightarrow RL pipeline improves *avg@8* by 1.3% but reduces *pass@1* by 12.2% at the 7B scale. This pattern indicates that SFT injects new knowledge into the model and raises the upper bound of its performance when multiple samples are allowed, whereas the subsequent RL phase, starting from an SFT-initialized

policy, tends to lose part of the exploration capability that is crucial for strong *pass@1* performance compared with directly training with on-policy RL. In practice, SFT encourages the model to follow a specific response style, which makes the response length and entropy during RL training concentrate in a relatively narrow range, thereby limiting exploration across diverse reasoning trajectories. In contrast, ADHint achieves the best results on both *pass@1* and *avg@8*. By explicitly accounting for difficulty, ADHint assigns an appropriate hint ratio to each sample and estimates fair relative advantages for each rollout, balancing exploration and imitation. As a result, the policy model simultaneously strengthens its reasoning ability and absorbs external knowledge from off-policy hints.

Training collapses when directly using full off-policy data. During our reimplementation of LUFFY [46], we observe that training collapses at an early stage (around 40 steps), accompanied by a sharp increase in both entropy and response length. We attribute this to over-imitation of the off-policy distribution, especially when there is a large discrepancy between the model that generates the off-policy data and the current policy. LUFFY feeds the complete off-policy trajectories into the mixed-policy GRPO objective as the off-policy term, while the other term remains the original on-policy GRPO objective. This forces the policy model to simultaneously fit two highly mismatched distributions, making training unstable and prone to collapse. In contrast, ADHint treats difficulty as a vital signal. It adjusts the hint ratio based on sample difficulty and estimates relative advantages based on rollout difficulty, achieving a better trade-off between learning from off-policy hints and maintaining exploratory on-policy reasoning.

Fixed hint ratios always lead to poor generalization. GHPO [25] and HintGRPO [12] share a similar design philosophy: they add hints with fixed ratios (e.g., 25%, 50%) only to the hardest problems. The key difference is that GHPO injects hints into the prompt and excludes them from the training loss, whereas HintGRPO treats hints as part of the response and includes them in the loss computation. In our experiments, we observe that GHPO exhibits large update magnitudes and highly unstable training, likely because the model is not truly learning the knowledge contained in the hints but instead adapting to an out-of-distribution reasoning pattern. In contrast, HintGRPO trains more stably and maintains a high average reward during training. However, as shown in Table 1, HintGRPO performs poorly on the benchmarks and shows limited generalization. The progressive hinting strategy for the hardest samples helps obtain positive rollouts, but it ignores sample difficulty and can provide excessive guidance, causing SFT-like overfitting to the hint distribution and weakening exploration. As a result, the model attains inflated training rewards under heavy hinting but fails to translate these gains into improvements on the benchmarks. By comparison, ADHint leverages a sample difficulty prior to assigning appropriate guidance to each example and uses low-variance update signals to gradually push the model’s capability boundary, enabling it to learn from off-policy data while preserving its inherent exploration.

Imbalanced intra-group advantage estimation leads to abnormal updates. Methods like StepHint [54] mix hint-rollouts with multiple fixed hint ratios, naive-rollouts, and ground-truth trajectories into a single group for advantage estimation without distinguishing among them. As shown in Figure 1b of the main text, this imbalanced intra-group estimation allows longer hint-rollouts with more positive trajectories to receive disproportionately large advantages, which biases policy updates toward imitating hints and leads to abnormal update behavior. This issue becomes more severe on ViRL-Hint17k, where the average hint length is about 3,100 tokens, while Qwen2.5-VL models typically generate only 400–500 tokens. In contrast, ADHint introduces AE-RDP, which estimates rollout advantages using the difficulty posterior evaluated from naive-rollouts and hint-rollouts, balancing learning between the two rollout types. CGM and Selective Masking further modulate token-level gradients within hints, which promotes more stable and reliable policy updates.

F Case Study

Figure 7 shows a representative training example. This case includes the extra prompt we added beyond the user query, which instructs the model to think before producing its response. For clarity, we omit this additional prompt in the subsequent cases. We see that the naive-rollout of the policy model fails to produce the correct answer. However, when we give the policy a hint taken from the complete off-policy reasoning trajectory, it continues the reasoning process and computes the final answer $z = 2\sqrt{15}$. In this way, the model not only learns the essential knowledge required to solve the problem from the hint but also improves its reasoning ability.

Figure 8 shows two representative benchmark examples. In the top case, the GRPO model lacks sufficient geometric knowledge and reaches an incorrect conclusion that *“a circle can tile a plane because it forms a complete 360-degree angle when placed around a point.”* In contrast, the ADHint model performs careful reasoning: it first interprets the meaning of *“tile a plane”* in the question, and then, through step-by-step reasoning, reaches the correct conclusion that *“the only shape that can tile a plane is the right triangle.”* In the bottom case, the GRPO model produces flawed reasoning, such as claiming that *“E is directly above B,”* and ultimately predicts the wrong option *“C”*. By comparison, the ADHint model conducts logically coherent reasoning: it first *“visualizes the solid shape”* and then gradually rules out incorrect options, finally selecting the correct answer *“D”*. These case studies indicate that GRPO fails to acquire the necessary external knowledge and exhibits weak reasoning ability, whereas ADHint treats difficulty as a key factor, learns essential knowledge from hints in a controllable manner, and develops more structured logical reasoning. This demonstrates ADHint’s strong ability to effectively integrate off-policy data into on-policy RL training.

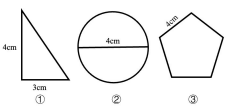
Case Study	
<p>Prompt: <system> You are a helpful assistant <user> Find z. Choices: (A) $2\sqrt{5}$ (B) $2\sqrt{6}$ (C) $2\sqrt{10}$ (D) $2\sqrt{15}$ ✓</p>	
<p>You FIRST think about the reasoning process as an internal monologue and then provide the final answer. The reasoning process MUST BE enclosed within <think> </think> tags. The final answer MUST BE put in \boxed{ }.</p> <p><assistant> <think></p>	
<p>Complete Off-Policy Reasoning Trajectory: Okay, let's see. I need to find the value of z in this triangle. Hmm, looking at the diagram, there's a big right triangle with some smaller right triangles inside. The big triangle has sides x, z, and the hypotenuse is $6 + 4 = 10$? Wait, no, wait. Wait, the hypotenuse of the big triangle is split into two parts: 4 and 6. Wait, no, maybe not. Let me look again. ... Thus, the value of z is $2\sqrt{15}$. \boxed{D}</p>	
<p>Naive-Rollout: Okay, let's start by looking at the image. We have a triangle with two right angles. The triangle is divided into two smaller right triangles. The key is that the two smaller triangles are similar to the larger triangle, and we can use the Pythagorean theorem in some way... Therefore, the correct answer is (C). </think> \boxed{C}</p>	
<p>Hint-Rollout: Okay, let's see. I need to find the value of z in this triangle. Hmm, looking at the diagram, there's a big right triangle with some smaller right triangles inside. The big triangle has sides x, z, and the hypotenuse is $6 + 4 = 10$? Wait, no, the hypotenuse is just the side opposite the right angle. So, the big triangle has sides z, x, and the hypotenuse is 10. The smaller triangle inside has sides 4, y, and x. And it's also a right triangle... So, the correct answer should be: [$z = 2\sqrt{15}$] </think> \boxed{D}</p>	

Fig. 7: A training example comparing naive-rollouts and hint-rollouts in ADHint.

Case Study

Case1:
According to the diagram, which of the following three shapes can tile a plane without gaps or overlaps?

A. ①: ✔
 B. ②:
 C. ③:
 D. Cannot be determined;
 E. No correct answer



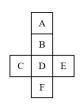
GRPO-Rollout:
 To determine which of the three shapes can tile a plane without gaps or overlaps, we need to consider the angles of their internal angles and how they can be combined to form a 360-degree angle around a point.

1. **Shape ①:** The right triangle
 ...
Shape ②: The circle with a diameter of 4 cm**
 A circle can tile a plane because it forms a complete 360-degree angle when placed around a point.
 ...
 It is clear that the circle (Shape ②) can tile a plane without gaps or overlaps.
 </think>
\boxed{B}

ADHint-Rollout:
 Okay, let's start by understanding the problem. We have three shapes: a right triangle, a circle, and a pentagon. The question is which of these shapes can tile a plane without gaps or overlaps. First, let's think about what it means to tile a plane...
 Therefore, the only shape that can tile a plane is the right triangle (Shape ①).
 The correct answer is A. ①.
 </think>
\boxed{A}

Case2:
 As shown in the diagram, after folding the net into a solid shape, the block opposite to block B is .

A. A:
 B. B:
 C. C:
 D. F: ✔
 E. No correct answer



GRPO-Rollout:
 To determine which block is opposite block B when the net is folded into a solid shape, we need to analyze the given net and imagine how the paper would fold.

1. The net has six squares labeled A, B, C, D, E, and F...
 Since B, D, and E form the top face, E is directly above B when folded. D is directly above C, and B is directly above F. Thus, block C is the one directly opposite to block B when the net is folded into a solid shape.
 Final answer: C
 </think>
\boxed{C}

ADHint-Rollout:
 Okay, let's start by understanding the problem. The image shows a net for a solid shape, and we need to identify which block is opposite to block B when the net is folded into a solid shape. The blocks are labeled A, B, C, D, E, and F. First, we need to visualize the solid shape...
 The other faces (A, C, D, E) are not directly opposite to B.
 Therefore, the block opposite to block B is F. So, the answer is D.
 </think>
\boxed{D}

Fig. 8: Two benchmark examples comparing ADHint with the GRPO baseline.